

SEARCH FOR A LIGHT STANDARD MODEL HIGGS BOSON IN THE $H \rightarrow WW^{(*)} \rightarrow e^+\nu e^-\bar{\nu}$ CHANNEL*

F. BEAUDETTE, C. CHARLOT, E. DELMEIRE[†], L. DOBRZYNSKI,
C. ROVELLI[‡], Y. SIROIS

Laboratoire Leprince-Ringuet, Ecole Polytechnique and IN2P3-CNRS, France

(Received November 15, 2006)

A prospective analysis for the discovery of a light Standard Model Higgs boson in the CMS experiment at the Large Hadron Collider is presented. The analysis focuses on the inclusive single production $p + p \rightarrow H + X$ and the Higgs boson decay channel $H \rightarrow WW^{(*)} \rightarrow e^+\nu e^-\bar{\nu}$, for a mass M_H in the range $120 < M_H < 160 \text{ GeV}/c^2$. A full simulation of the CMS detector response is performed and emphasis is put on the use of detailed electron reconstruction, as well as on realistic treatment of background contamination and systematics. A Higgs boson of mass $M_H \gtrsim 134 \text{ GeV}/c^2$ would be observed with a significance above 3 standard deviations in the $e^+\nu e^-\bar{\nu}$ channel alone for an integrated luminosity above 30 fb^{-1} .

PACS numbers: 14.80.Bn

1. Introduction

The Standard Model (SM) of electroweak interactions contains a unique physical Higgs boson whose mass, M_H , is a free parameter of the model. At the LHC pp collider, the inclusive single production reaction $p + p \rightarrow H + X$ followed by the decay in real or virtual W bosons, $H \rightarrow WW^{(*)} \rightarrow l^+\nu l^-\bar{\nu}$, can provide sensitivity over the full range of M_H favoured by direct and indirect constraints. In the intermediate mass range $2M_W \leq M_H \leq 2M_Z$ where the branching ratio of the SM Higgs boson into a W pair is close to one, the WW channel has been established to be a main discovery channel at the LHC [1, 2]. This paper presents a dedicated analysis for the CMS experiment to improve the sensitivity for a Higgs boson in the lower mass region of $M_H < 2M_W$ where the WW^* channel is likely to be complemented

* Presented at the "Physics at LHC" Conference, Kraków, Poland, July 3–8, 2006.

[†] Now at the Universidad Autónoma de Madrid.

[‡] Now at INFN Roma1.

by measurements in the ZZ^* channel [3]. The decay of both $W^{(*)}$ bosons into an electron and a neutrino are considered: $H \rightarrow WW^* \rightarrow e^+\nu e^-\bar{\nu}$ (in short $H \rightarrow 2e2\nu$). In the low Higgs mass region, the mean properties of kinematic observables for the signal depend on the Higgs mass M_H . Moreover, electron reconstruction issues become more critical due to the presence of at least one low P_T electron, generally coupled to a virtual boson W^* . More details concerning the analysis and an extended list of references can be found in [4].

2. Signal and background

The signal topology is characterized by two oppositely charged electrons at central pseudorapidities (η), large missing energy and no hard jet activity. Because the Higgs boson is a scalar, the W vector bosons are produced with anti-correlated spin projections and the decay electrons tend to be emitted collinear. The generated signal events comprise the main SM Model Higgs boson production processes at the LHC: gluon fusion $gg \rightarrow H$ and Vector Boson Fusion (VBF) $qq \rightarrow qqH$.

All sources of multi-lepton final states and missing transverse energy are potential background sources to the Higgs boson $2e2\nu$ signal. Processes involving the production of real or virtual vector boson pairs are particularly relevant. This includes direct electroweak production of $WW^{(*)}$, ZW and ZZ pairs, as well as the indirect W production via the top quark decay $t \rightarrow Wb$, in associated $Wt(b)$ and $t\bar{t}$ pair production processes. The inclusive $p+p \rightarrow Z+X$ and $p+p \rightarrow W+X$ production processes followed respectively by the decay modes $Z \rightarrow e^+e^-$ and $W \rightarrow e\nu$ have huge cross sections at the LHC and become dangerous when the Z^*/γ^* recoils against jets. In this case, the boost of the e^+e^- system closes up the opening angle between the electrons in the laboratory rest frame and the topology becomes similar to the signal topology if apparent missing transverse energy arises from a mis-measurement. Finally a “fake” dielectron with a missing transverse energy final state can be obtained in W +jet(s) events if one jet component is misidentified as an electron.

3. Event reconstruction and identification

The reconstruction of electrons uses information from the pixel detector, the silicon strip tracker and the electromagnetic calorimeter (ECAL). The detectors are immersed in a 4 T magnetic field parallel to the collider beam z axis, and provide good acceptance for electrons of $E_T^e > 5$ GeV up to a pseudorapidity $\eta^e = 2.5$ [5]. First, a pre-selection is made by imposing, in addition, track-supercluster energy-momentum and geometrical matching. Second, more stringent electron identification requirements are

imposed using observables able to discriminate real electrons from fake ones in QCD jets, originating for instance from $\pi^\pm\pi^0$ overlaps and γ conversions. To better deal with the different topologies of electrons in the detector, the classification of electron candidates according to their observable characteristics is used. A class- and η -dependent set of electron identification cuts has been used to preserve a good efficiency for real electrons while allowing for sufficient rejection of backgrounds when used in combination with electron isolation.

Electron candidates have to be isolated. Isolation criteria based either on tracker- or calorimeter-only information are applied. The optimization of these isolation cuts has been performed on the W +jet(s) sample with the goal to provide sufficient rejection of “fake” electron candidates from jet misidentification, while preserving a best possible electron detection efficiency.

The reconstruction of jets is fundamental for a powerful rejection of the $t\bar{t}$ background. An Iterative Cone Algorithm is used to reconstruct the jets from the energy deposits in the ECAL and HCAL.

The missing transverse energy (MET), is reconstructed by adding vectorially the transverse energy measured in ECAL and HCAL cells and the transverse energy of the reconstructed muons.

4. Event selection

A data reduction is first carried out in three steps. First, the $H \rightarrow WW^{(*)} \rightarrow 2e2\nu$ events need to pass the global Level 1 (L1) trigger, followed by the High Level Trigger (HLT). For the analysis, the HLT response is defined as the logical OR of the Single Electron Trigger (one isolated electron candidate with $P_T > 26$ GeV/ c) and the Double Electron Trigger (two isolated electron candidates with $P_T > 14.5$ GeV/ c). Second, events that pass the L1+HLT requirements and which contain exactly 2 isolated electrons with $E_T^e > 10$ GeV and $|\eta^e| < 2.5$ and coming from the same event vertex are selected. Finally, a Central Jet Veto (CJV) is applied against the $t\bar{t}$ and $Wt(b)$ backgrounds. These backgrounds are characterized by high P_T jets initiated by heavy quark flavours which are more centrally distributed than recoil jets in Higgs boson signal events. A kinematic selection is then performed. A sequence of cuts is introduced which are designed to preserve a good signal over background ratio while allowing for a high signal detection efficiency. The introduction of M_H -dependent cuts allows to follow the evolution of the event characteristics in the lower range of the Higgs boson mass spectrum. The cuts are adjusted to maximise the significance for a signal observation taking all statistical and systematic errors into account. The following kinematic cuts are applied:

- $25 < P_T^e(\text{highest}) < 50 \text{ GeV}/c$
(transverse momentum of the leading electron);
- $P_T^e(\text{lowest}) > 15 \text{ GeV}/c$
(transverse momentum of the second electron);
- $40 \text{ GeV} < \text{MET} < M_H c^2 - 50 \text{ GeV}$ (missing transverse energy);
- $\Delta\phi(e^+e^-) < 100^\circ$
(azimuthal angular separation between the electrons);
- $12 < M_{ee} < 40 \text{ GeV}/c^2$ (invariant mass of the e^+e^- system);
- $M_H/2 < M_T(WW) < M_H$ (reconstructed WW transverse mass).

The distributions of the angular separation between the electrons in the transverse plane is shown in Fig. 1 (a), for the Higgs boson signal and the backgrounds, together with the optimized cut values.

After the basic kinematic selection, about one hundred Z +jet(s) events are expected for 10fb^{-1} of integrated luminosity, compared to less than one hundred events expected for the Higgs boson signal. Hence, the basic kinematic selection has to be complemented. Dedicated cuts are introduced to reduce the contamination from the Z +jet(s) and W +jet(s) backgrounds to a manageable level.

The electrons originating from the decay of the Higgs boson tend to be emitted more centrally than those of the Z decay as seen in Fig. 1 (b). For the Z +jet(s) background, the observed MET results from mis-measurements of the recoiling jet(s). As a consequence, the MET is preferentially aligned with the hadronic jet at highest E_T^{jet} (leading jet). Moreover this observed MET does not in general balance the P_T of the e^+e^- system. This is in

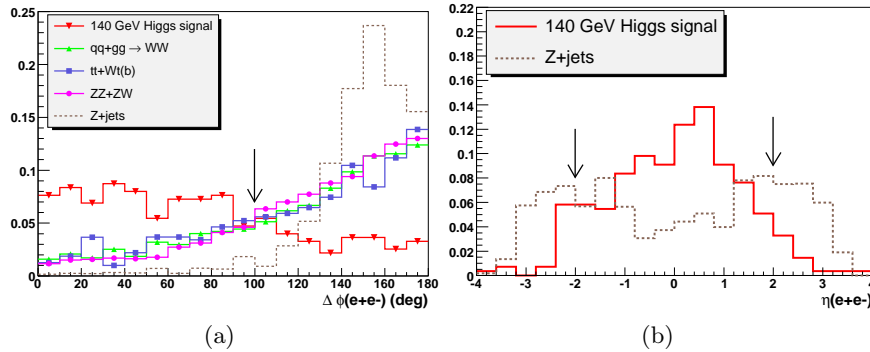


Fig.1. (a): angular separation between the electrons in the transverse plane; (b): pseudorapidity of the e^+e^- system; The vertical arrows indicate the cut positions for the basic $140 \text{ GeV}/c^2$ Higgs boson signal selection. The distributions are shown after data reduction.

contrast to the expectations for the Higgs boson signal. For the Higgs boson signal events, the MET direction in the transverse plane is in general well separated from the direction of the leading jet and the MET measures well the neutrinos from the W decays. Hence, the following cuts are applied:

- $|\eta(e^+e^-)| < 2$;
- $P_T(e^+e^-) - \text{MET} < 15 \text{ GeV}$;
- $\Delta\phi(\text{MET-leading jet}) > 40^\circ$.

All together, 35 $Z + \text{jet(s)}$ events are expected for 10 fb^{-1} .

The $W + \text{jet(s)} \rightarrow e\nu + \text{jet(s)}$ events where an electron is misidentified in a jet have measured properties similar to those of the Higgs boson signal; two “electrons” and missing transverse energy. Therefore, electron selection plays a major role in the suppression of this background. The two electron candidates in the $W + \text{jet(s)}$ background tend to be more separated in η than for the Higgs boson signal. This is because the fake electron in $W + \text{jet(s)}$ events often appears in low E_T misidentified jet at larger pseudorapidities. Hence, further rejection is obtained by imposing $|\Delta\eta(e^+e^-)| < 1$. The expected number of $W + \text{jet(s)} \rightarrow e\nu + \text{jets}$ events for 10 fb^{-1} integrated luminosity is < 6 .

5. Results

Fig. 2(a) shows the reconstructed WW transverse mass distribution expected in CMS for a typical single experiment with 10 fb^{-1} of integrated luminosity. An excess of event is visible above the sum of background contributions. The estimator S_{cP} , based on the counting method, is chosen

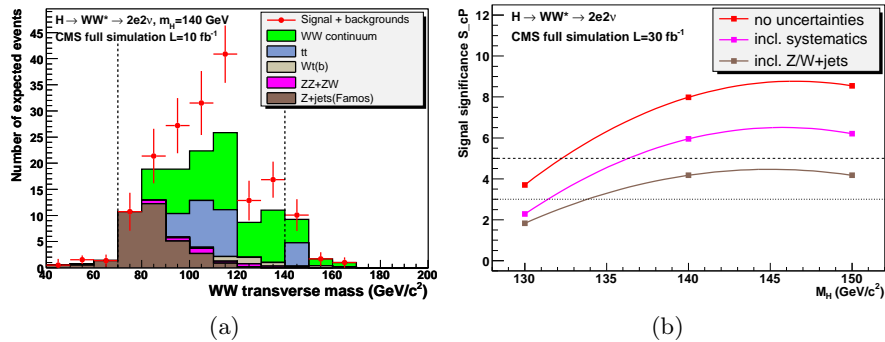


Fig. 2. (a): Reconstructed WW transverse mass distribution for 10 fb^{-1} integrated luminosity for (the sum of) the background contributions (histograms) and for the signal plus background observation (dots) for a $140 \text{ GeV}/c^2$ Higgs boson signal; (b): Significance for 30 fb^{-1} luminosity as function of the Higgs boson mass M_H with and without systematic uncertainties and expected $W/Z + \text{jet(s)}$ background.

to extract the signal significance. Fig. 2(b) shows the significance expected for 30 fb^{-1} of luminosity. The effect on the background estimation of the systematics is of the order of 6%–7%. A 3σ observation can be achieved for $M_H \gtrsim 134 \text{ GeV}/c^2$ with a 30 fb^{-1} luminosity. This provides an excellent complementarity with the ZZ^* channel. A stand-alone discovery (above 5 standard deviations) can be established for masses in the range 139 to 150 GeV/c^2 for \mathcal{L} above 60 fb^{-1} (*cf.* Fig. 7(b) in [4]).

We would like to thank P. Busson, A. Nikitenko and I. Puljak for their interest in this $WW^{(*)}$ analysis and several useful discussions. Our thanks go also to the other members working on the $H \rightarrow WW^{(*)} \rightarrow l\nu l\nu$ channel, G. Davatz, V. Drollinger, A.S. Giolo-Nicollerat and M. Zanetti for their collaboration.

REFERENCES

- [1] M. Dittmar, H.K. Dreiner, *Phys. Rev.* **D55**, 167 (1997); M. Dittmar, H.K. Dreiner, LHC Higgs Search with $l^+\nu l^-\bar{\nu}$ Final States, CMS NOTE-1997/083 (1997).
- [2] G. Davatz, M. Dittmar, A.-S. Giolo-Nicollerat, Standard Model Higgs Discovery Potential of CMS in the $H \rightarrow WW \rightarrow l\nu l\nu$ Channel, CMS NOTE-2006/047 (2006).
- [3] S. Baffioni *et al.*, Discovery Potential for the SM Higgs Boson in the $H \rightarrow ZZ^{(*)} \rightarrow e^+e^-e^+e^-$ Decay Channel, CMS NOTE-2006/115 (2006).
- [4] F. Beaudette *et al.*, Search for a Light Standard Model Higgs Boson in the $H \rightarrow WW^{(*)} \rightarrow e^+\nu e^-\bar{\nu}$ Channel, CMS NOTE-2006/114 (2006), CMS Physics Technical Design Report, Volume II, CERN-LHCC-2006-021.
- [5] S. Baffioni *et al.*, Electron Reconstruction in CMS, CMS NOTE-2006/040 (2006).